Smoke Wire Visualization of Unsteady Separation Over an Oscillating Airfoil

Jong Seong Kim* and Seung O. Park†
Korea Advanced Institute of Science and Technology, Seoul, Korea

STUDIES of unsteady separation have received considerable attention, particularly in connection with the problem of unsteady airfoil stall. One typical example is the dynamic stall phenomenon of an oscillating airfoil. Previous work[1-3] was mainly concerned with the aerodynamic events when the amplitude of oscillation was very large to ensure a "deep" dynamic stall to occur. In a deep dynamic stall, the shedding mechanism of "dynamic stall vortex" from the leading-edge region is believed to play a crucial role.

Evidently, unsteady boundary-layer separation is one of the most important features involved in the dynamic stall phenomenon. However, the theoretical understanding of unsteady boundary-layer separation[4,5] has not explicitly touched on the dynamic stall phenomenon. This is probably because the separation in dynamic stall is so massive: the whole upper surface of the airfoil is covered with a wake in those circumstances.

The primary intention of this Note is to examine the separation phenomenon of an airfoil that is oscillating with a relatively small amplitude. Results of our first-phase efforts to measure the wakes of such a flow are reported elsewhere;[6] that study clearly suggested the periodic occurrence of unsteady separation. In the present Note, we make available the results of our second-phase efforts to visualize the unsteady separation phenomenon over an airfoil surface, when the airfoil is executing a pitching oscillation with a relatively small amplitude. The purpose of the present investigation is 1) to scrutinize the chronology of events occurring during a period of oscillation, and 2) to interpret the unsteady separation observed in the visualization study, aided by the unsteady boundary-layer separation theory.

Experiments

The experimental setup used for the present study was the same as the one reported earlier.[6] A NACA 0012 airfoil of 10-cm chord and 19.8-cm span was mounted horizontally in an open circuit, 20 cm × 30 cm wind tunnel. The freestream turbulence level was 0.4%.

Pitching oscillation about the quarter-chord axis was driven by a variable-speed ac motor and a crank-connecting rod mechanism. In order to generate smoke, a nichrome wire of 0.1-mm diam was installed vertically at the location 15 mm forward of the leading edge in the centerplane of the test section. Another wire was installed spanwise over the upper surface at the 0.9 chordwise station from the leading edge to visualize the near surface flow. The height of the wire from the airfoil surface was 1 mm.

Still photographs were taken by a 35-mm Pentax SLR camera equipped with the standard lens (f1.4). Lighting was provided by a stroboscope having a 25-μs-flash duration. The stroboscope was synchronized with a trigger pulse produced at a predetermined instantaneous angle of attack.

The experiments were performed for two different reduced frequencies: $K = 0.09$ and 0.20. The reduced frequency K is defined as $K = \omega C/2U_\infty$, where ω is the circular frequency, C is the chord length, and U_∞ is the freestream velocity. In both cases, the Reynolds number based on the chord length was 27,000.

The mean incidence angle and the oscillation amplitude were set at 0 and 7.4 deg, respectively; thus, the instantaneous angle of attack α can be described as $\alpha = 7.4 \sin\omega t$ in degrees.

Results and Discussion

Figures 1a–1i show the chronological flow patterns around the airfoil for $K = 0.20$ at various instantaneous angles of attack. The brighter white streaks near the airfoil surface and/or in the central part of the wake were generated from the nichrome wire installed over the upper surface of the airfoil at $0.9C$. At $\alpha = 6.4$ deg (Fig. 1a) and at $\alpha = 7.4$ deg (Fig. 1b) (which is the maximum instantaneous angle of attack), a thin layer of reversed flow is seen in the downstream portion of the airfoil, creeping up toward the leading edge. The wake vortex patterns are similar to the characteristics of the Karman vortex shedding. This indicates that the boundary layer on the airfoil is laminar.[3] It is also recognized that the front of the near surface streak of Fig. 1c has gone further upstream than that of Fig. 16. This implies that the front of the reversed flow has

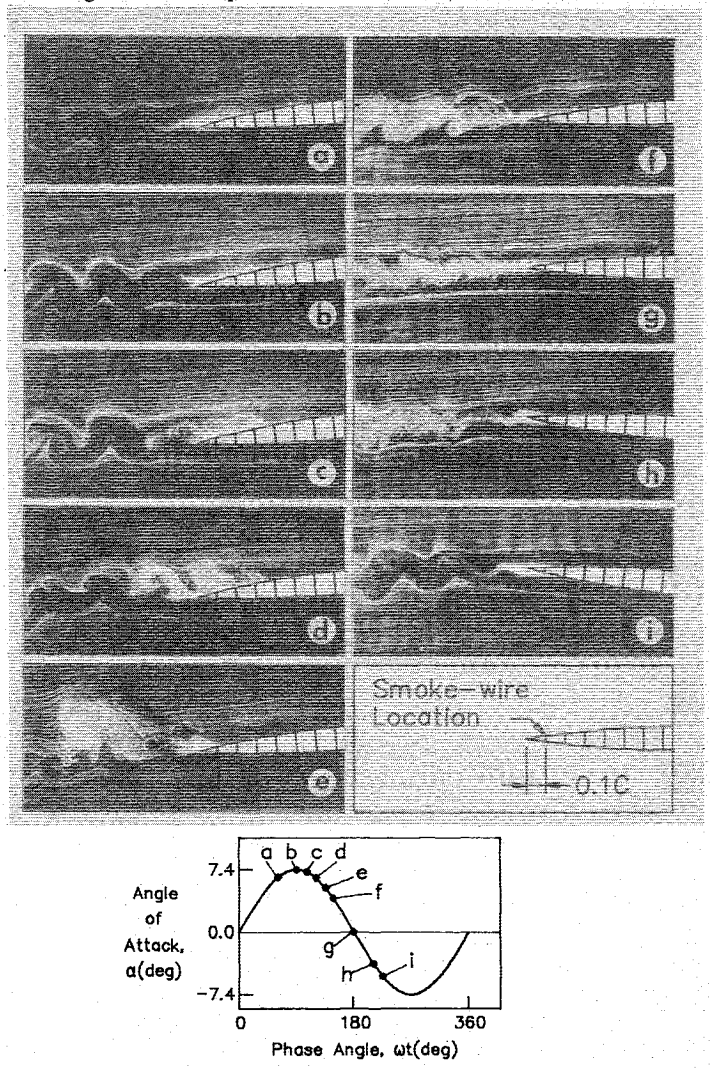

Fig. 1 Chronological flow patterns ($K = 0.20$): a) $\alpha = 6.4$ deg, $\omega t = 60$ deg; b) $\alpha = 7.4$ deg, $\omega t = 90$ deg; c) $\alpha = 7.1$ deg, $\omega t = 105$ deg; d) $\alpha = 6.4$ deg, $\omega t = 120$ deg; e) $\alpha = 5.2$ deg, $\omega t = 135$ deg; f) $\alpha = 3.7$ deg, $\omega t = 150$ deg; g) $\alpha = 0$ deg, $\omega t = 180$ deg; h) $\alpha = 3.7$ deg, $\omega t = 210$ deg; i) $\alpha = -5.2$ deg, $\omega t = 225$ deg.

Received March 11, 1987; revision received Dec. 1, 1987.

*Research Assistant, Aerospace Program, Department of Mechanical Engineering.

†Associate Professor, Aerospace Program, Department of Mechanical Engineering. Member AIAA.

moved upstream even as the angle of attack has decreased. When the front of the reversed flow reaches its uppermost position (about $0.6C$ from the leading edge), the viscous shear layer thickens rapidly and becomes discretized by the development of numerous vortices (Fig. 1c). Subsequently, these vortices are broken down and transformed into the turbulent vortical structures (Fig. 1d). It seems that the unsteady separation of laminar boundary layer has occurred. The enlarged vortical structure over the airfoil surface in Fig. 1d is seen to explode into the wake to a width about as large as one-third of the chord (Fig. 1e). A plausible reason for this is that there exists no solid boundary to inhibit the growth of the structure in the wake when it is washed off the trailing edge. A very similar phenomenon of bursting has been observed by Koromilas and Telionis.[5] Figures 1f and 1g display the wake developments at later times. It is noted that the wakes in these figures are fully turbulent. When the airfoil angle of attack increases in the opposite direction, the reversed flow region starts to reappear. In Fig. 1h, a thin bright white streak over the lower surface is clearly visible. Notice that the smoke wire is located over the upper surface. In Fig. 1i, it is discernible that the wake becomes wavy and relaminarizes. Since the airfoil is symmetric and the mean incidence angle is zero, the chronological flow patterns for negative angles of attack (i.e., $\omega t = 180$ deg ~ 360 deg) are substantially the same as those demonstrated in the frames of Fig. 1a to 1g.

In addition to the occurrence of unsteady separation, the present studies reveal another interesting feature. It is significant to watch that the wake undergoes transition and reverse transition during a period of oscillation. As part of these studies, we made extensive steady-state flow visualizations of wakes when the airfoil was stationary. Under the steady-state conditions, at $\alpha = 0$ deg, the wake was well organized into a Karman vortex street, whereas at $\alpha = 7.4$ deg, it was fully turbulent. On the contrary, the unsteady wake at the instantaneous angle of attack of 7.4 deg is organized into periodic structures (Fig. 1b). Based on the limited information available from the present experimental studies, we are not able to ascertain whether or not the unsteady separation is essential for the wake to undergo transition. It is clear, however, that the wake transition from laminar to turbulent, as demonstrated in Fig. 1, is attributable to unsteady separation.

For the lower reduced frequency of $K = 0.09$, the sequence of events is the same as that for $K = 0.20$. However the phase angles corresponding to the similar events are different. It should be noted that for $K = 0.09$ the unsteady separation occurs at $\omega t \cong 75$ deg ($\alpha \cong 7.1$ deg) when the airfoil incidence is increasing (Fig. 2). On the contrary, for $K = 0.20$, the similar event occurs at $\omega t \cong 105$ deg ($\alpha \cong 7.1$ deg) when the airfoil incidence is decreasing (Fig. 1). This suggests that the time required for the unsteady boundary-layer fluid to react to the change of the outer flow conditions is principally governed by the flow time scale C/U_∞. Figure 3 depicts the relationship between the phase angle at which the unsteady separation occurs and the reduced frequency K. The data for $K = 0.13$ was evaluated from the hot-wire measurements.[6] Obviously, as K increases, the phase angle at which unsteady separation occurs increases. The effect of the reduced frequency on the delay of dynamic stall[2] is qualitatively similar to that described in the present observations. If an assumption can be made that the phase angle variation with K can be linearly extrapolated to the limit of quasisteady case ($K \to 0$), then $(\omega t)_{K\to 0}$ can be located on the diagram (Fig. 3). Using this, a time delay in the response of boundary-layer separation can be estimated. The linear relationship between ωt and K points to an expression for the time delay Δt as

$$\omega \Delta t / K = \text{const} \qquad (1)$$

When the constant in Eq. (1) is evaluated from the data of Fig. 3, the dimensionless time delay $U_\infty \Delta t/C$ becomes approximately 3. For the case of an impulsively started circular cylinder, the dimensionless time for the boundary layer to break down was approximately 1.5 as reviewed in Telionis.[7] Computations performed by Mehta and Lavan[8] for the flow around an impulsively started airfoil at $\alpha = 15$ deg and $Re = 1000$ showed that the bursting of separation bubble appeared at dimensionless time of 2.2. In view of the fact that large differences exist in flow geometry between the present case and the two cases cited above, a direct quantitative comparison of time delay is of little physical significance. We assert, however, that the orders of magnitude of those values are in fair agreement.

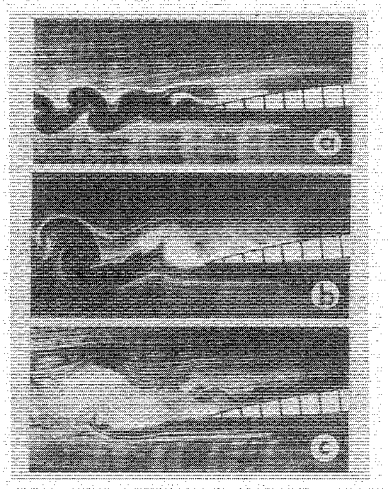

Fig. 2 Chronological flow patterns ($K = 0.09$): a) $\alpha = 6.4$ deg, $\omega t = 60$ deg; b) $\alpha = 7.1$ deg, $\omega t = 75$ deg; c) $\alpha = 7.4$ deg, $\omega t = 90$ deg.

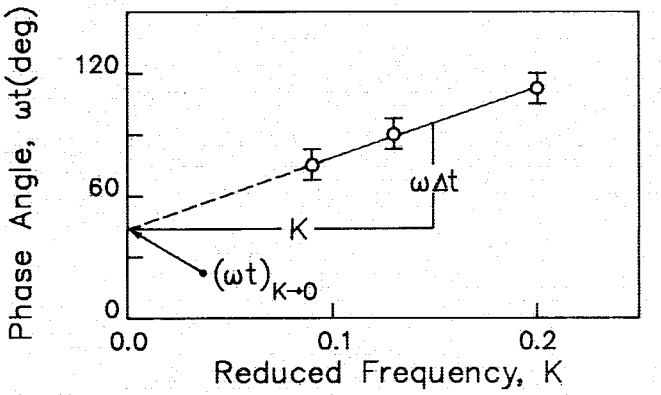

Fig. 3 Phase angle of unsteady separation.

The unsteady separation over an oscillating airfoil surface may well be considered as the "upstream moving separation" of Refs. 4 and 5. The visualization for the sequence of unsteady separation over "model B" of Koromilas and Telionis[5] (Fig. 28 of Ref. 5) demonstrates that the thin layer of reversed flow moves upstream up to its uppermost position. As the uppermost position is reached, the boundary layer thickens rapidly. The rapid thickening of the boundary layer or eruption into a violent wake appears to have been substantially accomplished when the separation point catches up with the front of the reversed flow region. These previous findings are in qualitative agreement with the present observations. The sequence of events displayed in Figs. 1e–1g is supportive of our speculation that the whole reversed flow region turns into the separated wake when the front of the reversed flow region reaches its uppermost position. However, in the present visualization, the separated region downstream of the separation points is virtually indistinguishable from the thin layer of reversed flow. Consequently, it will be necessary to conduct more elaborate visualization experiments to identify correctly the separated region and the thin layer of reversed flow. These experiments will deepen our knowledge of unsteady boundary-layer separation over an oscillating airfoil.

Summary

The chronological flow patterns around an airfoil that was oscillating in pitch with a relatively small amplitude were investigated using a smoke wire technique.

The unsteady separation observed in the present experiment was seen to be accomplished as the front of the reversed flow region reached its uppermost position. The separation did not necessarily take place when the instantaneous angle of attack α reached its maximum value. The instantaneous angle of attack at which the separation took place was seen to depend on the reduced frequency K. For flows with a larger K, the specific event of separation occurred at a larger phase angle ωt.

References

[1]Johnson, W. and Ham, N. D., "On the Mechanism of Dynamic Stall," *Journal of the American Helicopter Society*, Vol. 17, Oct. 1972, pp. 36–45.

[2]McCroskey, W. J., Carr, L. W., and McAlister, K. W., "Dynamic Stall Experiments on Oscillating Airfoils," *AIAA Journal*, Vol. 14, Jan. 1976, pp. 57–63.

[3]McAlister, K. W. and Carr, L. W., "Water Tunnel Visualizations of Dynamic Stall," *ASME Transactions, Series I—Journal of Fluids Engineering*, Vol. 101, Sept. 1979, pp. 376–380.

[4]Sears, W. R. and Telionis, D. P., "Boundary-Layer Separation in Unsteady Flow," *SIAM Journal on Applied Mathematics*, Vol. 28, Jan. 1975, pp. 215–235.

[5]Koromilas, C. A. and Telionis, D. P., "Unsteady Laminar Separation: an Experimental Study," *Journal of Fluid Mechanics*, Vol. 97, 1980, pp. 347–384.

[6]Park, S. O. and Kim, J. S., "Wake Measurements of an Oscillating Airfoil," *Proceedings of the International Symposium on Refined Flow Modelling and Turbulence Measurements*, Univ. of Iowa, Iowa City, IA, 1985, pp. D16-1–D16-10.

[7]Telionis, D. P., *Unsteady Viscous Flows*, Springer-Verlag, New York, 1981.

[8]Mehta, U. B. and Lavan, Z., "Starting Vortex, Separation Bubbles and Stall: a Numerical Study of Laminar Unsteady Flow around an Airfoil," *Journal of Fluid Mechanics*, Vol. 67, Pt. 2, 1975, pp. 227–256.

Viscous Effects on the Resonance of a Slotted Wind Tunnel Using Finite Elements

In Lee*

Stanford University, Stanford, California

Nomenclature

a_0 = speed of sound of fluid medium
a_e = effective speed of sound, $a_0\sqrt{1-M^2}$
h = half-width of slot
i = $\sqrt{-1}$
k = reduced frequency, $\omega h/a_0$
l = tunnel wall thickness
m = $M/1-M^2$
M = freestream Mach number
p = perturbation pressure
p_s = mean pressure
p^* = nondimensional perturbation pressure, p/p_s
s = shear wave number, $h\sqrt{\rho_s\omega/\mu}$
u = nondimensional velocity in $\bar{x}$ direction (Fig. 2)
$\bar{u}$ = velocity component in $\bar{x}$ direction (Fig. 2)
v = nondimensional velocity in $\bar{y}$ direction (Fig. 2)
w = nondimensional velocity in z direction (Fig. 2)
γ = ratio of specific heat
λ = eigenvalue
μ = viscosity coefficient of fluid
ρ = density, $\rho_s(1+\rho^*)$
ρ_s = density in undisturbed stream
ρ^* = nondimensional perturbation density
ω = angular frequency

Received May 26, 1987; revision received Feb. 22, 1988.

*Graduate Student, Department of Aeronautics and Astronautics; currently Assistant Professor at Department of Mechanical Engineering, Korea Advanced Institute of Science and Technology. Member AIAA.

I. Introduction

MODEL flutter and oscillatory airload measurements will be affected by coupling with an acoustic vibration mode when the model frequency is near a tunnel resonance frequency. Widmayer, Clevenson, and Leadbetter[1] conducted some experiments to measure the oscillatory aerodynamic forces and moments acting on a rectangular wing. The test results were in considerable error near the tunnel resonant frequency. Therefore, we want to predict the wind-tunnel resonant frequency accurately. Davis and Moore[2] and Acum[3] have obtained the resonance frequencies for a rectangular cross section. Lee[4] has obtained the resonance frequencies for an arbitrarily shaped cross section by using finite elements. These previous investigators have obtained the resonance frequencies without considering viscosity effects in the slot.

The effects of viscosity increase when the slot width becomes small. Many wind tunnels have a very small slot open area ratio (0–5%). When the slot width becomes small, wave propagation through the slot will be affected by the slot boundary layer. Tijdeman[5] has studied the propagation of sound waves in cylindrical tubes both analytically and numerically. The velocity-pressure ratio that is obtained by extending Tijdeman's approach to the slot is used as a boundary condition on the slot.

A finite-element treatment of the damping problem was given recently. Craggs[6] considered a damped acoustic system to study the performance of a muffler by the finite-element method. Kagawa et al.[7] considered an axisymmetric acoustic transmission with boundaries of acoustic impedance. Joppa and Fyfe[8] studied the impedance properties of arbitrarily shaped cavities with dissipative boundaries.

We will confine our concern to the wind tunnel that does not have a plenum chamber to simplify the problem, and we will discuss the case in which the slot width is very small to consider viscosity effects.

II. Governing Equation and Boundary Conditions

For a test section of a wind tunnel shown in Fig. 1, the following governing equation can be obtained from Ref. 4:

$$p_{xx} + p_{yy} + (\omega/a_e)^2 p = 0 \tag{1}$$

The boundary condition on the solid wall is given as

$$\frac{\partial p}{\partial n} = 0 \tag{2}$$

The boundary condition on the slot can be derived from the following linearized momentum equation:

$$\left(\frac{\partial}{\partial t} + U_\infty \frac{\partial}{\partial z}\right) u_n = -\frac{1}{\rho}\frac{\partial p}{\partial n} \tag{3}$$

where n is in the direction of the outward normal. For a narrow slot, the velocity component in the z direction inside a slot is very small ($U_\infty \approx 0$). Then, for a sinusoidal motion, we get

$$\frac{\partial p}{\partial n} = -i\rho\omega A p \tag{4}$$